Indoor Positioning Using Correlation Based Signal Analysis and Convolutional Neural Networks

Ivo Bizon*, Ahmad Nimr*, Gerhard Fettweis* and Marwa Chafii†‡
*Vodafone Chair Mobile Communications Systems, Technische Universität Dresden (TUD), Germany
{ivo.bizon, ahmad.nimr, gerhard.fettweis}@ifn.et.tu-dresden.de
†Engineering Division, New York University (NYU), Abu Dhabi, UAE
‡NYU WIRELESS, NYU Tandon School of Engineering, New York, USA
marwa.chafii@nyu.edu

***Abstract*—Positioning algorithms are designed based on location related information contained in received signals, these can be propagation delay, angle of arrival, and received power. However, regardless of the positioning parameter, low-complexity linear position estimators provide reliable and accurate results only under line-of-sight propagation conditions. Hence, this paper proposes an alternative position information parameter based on the correlation of signals received at several sensing units. A low-complexity convolutional neural network uses this novel parameter for estimating the source coordinates. A simulated indoor environment based on ray tracing has been employed to compare the localization performance of the proposed approach against classical positioning schemes under a common simulation framework. The results indicate that an accurate yet low-complexity positioning solution can be achieved in multipath propagation scenarios where traditional schemes based on time-difference-of-arrival and received signal strength usually present limited performance. Furthermore, guidelines for selecting system parameters that improve the positioning accuracy of the proposed scheme are presented.**

***Index Terms*—Positioning and localization, wireless sensor network (WSN), deep learning, integrated sensing and communication (ISAC).**

I. Introduction

Perspectives on the sixth generation (6G) of mobile communications seem to agree on a strong interest on accurate indoor positioning techniques, since it has a central role in enabling, for example, the *connected intelligence* concept, where accuracy levels must be in the order of tens of centimeters [1]. This trend can be attributed to the increasing number of envisioned use cases in future wireless networks, where location information can be exploited for enhancing network services and the overall performance [2]. Still within the foreseen technologies in 6G networks, integrated communications and sensing (ISAC) seeks to combine these two services by employing techniques which allow the simultaneous use of spectrum and hardware for either communications or sensing tasks [3], [4]. Furthermore, location awareness can help to pave the way towards proactive flexible radio resource management by the network. Nevertheless, a set of challenges must be addressed to achieve the envisioned integration between the two services. These include: to develop a joint waveform design and signaling protocol that can tuned to achieve both sensing and communications performance requirements, and to advance in the modeling of the wireless channel models that are not averaged over the spatial domain, i.e., geometric channel models.

The localization service of an active signal source can be classified into two main categories: *self-positioning* and *remote-positioning*. The first corresponds to the case where a mobile device, i.e. a signal source, wants to know its position within a global, or local, coordinate system. Hence, it processes the signals incoming from several devices at known locations for estimating its own position. In contrast, remote-positioning often assumes a wireless sensor network (WSN), where multiple sensing units (SUs) are connected to a central unit (CU). The SUs collects incoming signals from the sources(s), and send them to the CU, where source coordinates are estimated. This work focuses on remote-positioning.

Our contributions can be summarized as follows: We present an investigation of an alternative positioning technique which exploits the synchronization among SUs for defining a positioning information feature named position information correlation matrix (PICM). This feature is employed in a deep learning (DL)-based localization approach, which is able to outperform classical positioning techniques that rely solely on received signal strength (RSS) or time difference of arrival (TDoA) for source coordinate estimation. Throughout this work the device to be localized is named source. The definition of the PICM, and how the system sampling frequency and transmit signal auto-correlation properties affect the positioning performance are explored. Recommendations for the obtaining ideal values are also devised. The positioning performance is investigated under a scenario whose propagation effects are based on a ray tracing software, which provides accurate spatial channel information.

The remainder of the paper is organized as follows: Section II presents the system model. Section III describes the main contributions of the paper. Section IV analyses the performance of the localization schemes under a ray tracing based channel model. Finally, the paper is concluded in Section V.

II. System Model

In an indoor area where the positioning service is to be available, N clock synchronized SUs are placed in fixed locations, and all are connected to a CU, thus forming a

WSN. The spatially distributed SUs listen to the channel for a positioning preamble transmitted by the source device that is to be localized. Once this preamble is identified, the SUs send to the CU the in-phase and quadrature (I/Q) samples corresponding to the preamble. Finally, the CU uses these signals for source position estimation.

The band limited wireless channel model is defined as a superposition of incoming signal components that traveled through multiple propagation paths; and therefore, they arrive at the receiver with different delays, amplitudes and phases. Moreover, when either transmitter or receiver moves, or the environment is modified, these quantities vary over time. Therefore, the it can be represented as a time-variant low pass filter from the receiver perspective [5]. Thus, the complex baseband channel impulse response observed at the j-th SU can be expressed by

$$h_j(t,\tau) = \sum_{l=0}^{L(t)-1} \alpha_l(t)\delta\left(t-\tau_l(t)\right)\exp\left(-j2\pi f_c \tau_l(t)\right), \quad (1)$$

where $L(t)$ represent the total number of significant propagation paths, $\alpha_l(t)$, $\tau_l(t)$ represent the amplitude and delay associated with the l-th path, respectively, f_c denotes the carrier frequency, and $\delta(\cdot)$ the Dirac delta function.

Equation (1) presents a continuous time formulation, but in digital receivers the received signal is sampled at a given sampling frequency $f_s = 1/T_s$ Hz, where T_s is sampling time interval in seconds, giving rise to the band limited representation of the wireless channel. When the difference between delays from propagation paths is smaller than T_s, these are vectorially-combined into a single component. The equivalent channel in frequency domain is given by

$$H_j(k) = \sum_{l=0}^{L-1} \alpha_l \exp\left(-j2\pi \frac{k}{K} f_s \tau_l\right)\exp\left(-j2\pi f_c \tau_l\right), \quad (2)$$

where $H_j(k)$ is the channel gain at frequency $f_c + \frac{k}{K} f_s$ Hz, and $k \in \{-K/2, \ldots, K/2-1\}$ is the frequency bin index. The time dependency has been dropped meaning that this represents an instantaneous channel frequency response.

In summary, the wireless channel between source and SU can be characterized by a combination of parameters, such as α_l and τ_l, which are dependent on the positions of both devices. In this case, the channel model in (2) is quite useful for the numerical analysis of positioning systems, since it allows us to explore the performance of different positioning parameters under a common model. Furthermore, it gives us the ability to investigate the effects of the bandwidth limitation when the ray tracing software is used to obtain the exact path delays, gains and phases.

III. Correlation Matrix Based Positioning Algorithm

A. Mathematical Definitions

Let the Euclidean distance between the signal source and j-th SU be defined as

$$d_j = \sqrt{(x-x_j)^2 + (y-y_j)^2}, \quad (3)$$

where the pairs $(x,\, y)$ and $(x_j,\, y_j)$ are the Cartesian coordinates of the signal source and j-th SU, respectively.

Let

$$\mathbf{Z} = \left[Z_0(k),\, \cdots,\, Z_{N-1}(k)\right] \in \mathbb{C}^{K\times N} \quad (4)$$

be a matrix containing in each column

$$Z_j(k) = H_j(k)X(k) + W_j(k), \quad (5)$$

which is a K-long complex-valued vector with the samples of the received signal at the j-th SU in frequency domain. $H_j(k)$ and $X(k)$ are the channel impulse response and the transmit signal in frequency domain, respectively, and $W_j(k)$ is additive white Gaussian noise (AWGN). Note that a periodic transmission of a positioning signal is assumed, such that the received signal $z_j[n] = h_j[n] \circledast x[n] + w_j[n]$ has period $N_s = K$, where $\circledast$ represents the circular convolution, and N_s is the length of the transmit signal. Thus, the correlation matrix of the received signals is given by

$$\mathbf{Q} = \frac{1}{K}\mathbf{Z}^{\mathrm{H}}\mathbf{Z} \in \mathbb{C}^{N\times N}, \quad (6)$$

where $(\cdot)^{\mathrm{H}}$ represents Hermitian transpose [6]. Note that the RSS (dBm) measurement at the j-th SU is obtained from the diagonal elements as

$$P_j = 10\log_{10}\left([\mathbf{Q}]_{jj}\right) + 30, \quad (7)$$

where $[\cdot]_{ij}$ represents the matrix indexing operator. The PICM is given by

$$\mathbf{Q}_{\mathrm{PICM}} \triangleq 10\log_{10}\left(|\mathbf{Q}|\right). \quad (8)$$

Let the absolute differential source-SU distance between the i-th and j-th SUs be represented by

$$\Delta d_{ij} = |d_i - d_j|, \quad (9)$$

and the correlation spatial resolution be defined as

$$R = \frac{c}{B}, \quad (10)$$

where c is the speed of light and $B = f_s$ is the system bandwidth.

B. Positioning Parameter Design

Assuming that the SUs are synchronized, as it is required for TDoA-based positioning, the CU is able to coherently exploit the position related information contained in the received I/Q samples. Directly feeding the I/Q samples collected by the SUs to a neural network would theoretically yield the best positioning performance, since all the available location information, i.e., α_l and τ_l, are contained in these raw signals. Nevertheless, the dimensionality of the input, i.e., $N \times N_s \times 2$, quickly demonstrates that this approach is unfeasible, and one of the reasons is known as the curse of dimensionality [7], which states that the number of training examples required for obtaining a well-fitting model grows exponentially with the input size. Hence, we propose to represent the source location with the PICM, which reduces the input dimensionality to $N \times N$, but still maintains more information when compared to solely employing RSS or TDoA.

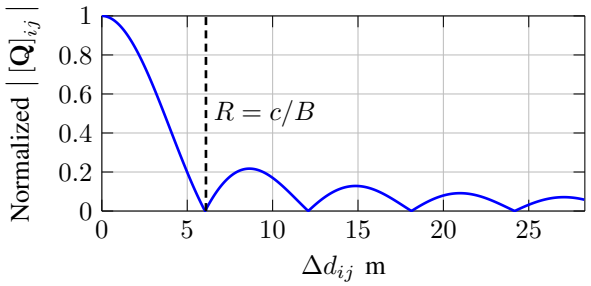

Fig. 1: Normalized correlation between the received signals at the i-th and j-th SUs as a function of Δd_{ij}. The spatial resolution is indicated by the dashed line, where $B = 50$ MHz, and a Zadoff-Chu sequence is employed as transmit signal.

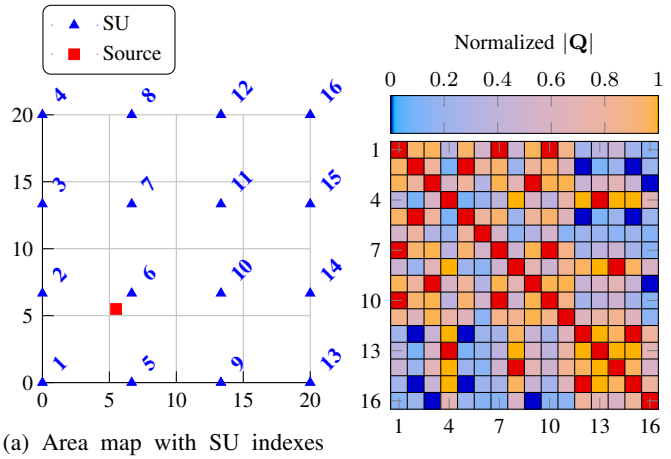

(a) Area map with SU indexes and source.

(b) Normalized PICM.

Fig. 2: Scenario illustrating that maximum correlation is observed in off-diagonal elements that corresponds to $\Delta d_{ij} = 0$, and minimum correlation is observed when $\Delta d_{ij} = mR$. For the sake of visualization, $B = c/\Delta d_{2,12}$ Hz, and a pure line-of-sight (LoS) channel was assumed between the source at [5.5, 5.5] and SUs.

The choice of transmit signal plays a role on the PICM representation ability. Ideally, the discrete-time autocorrelation function of the positioning pilot signal should be a Kronecker delta function. This can be achieved with cyclic transmission of spreading sequences, but cannot be attained in the aperiodic case [8]. Zadoff-Chu sequences are a good example of such sequences, and they are well-known for being employed as a pilot signals in multiple wireless communications standards. Hence, these are employed in this paper as positioning pilot signal. For N_s even, the sequence is given by

$$x_{\mathrm{ZC}}[n] = \exp\left(j\pi n^2/N_s\right), \tag{11}$$

where N_s is the length of the sequence. Figure 1 shows the normalized correlation between the received signals at the i-th and j-th SUs as a function of Δd_{ij} assuming this sequence as positioning pilot signal.

As aforementioned, the j-th SU RSS is obtained via (7). However, further location information other than the RSS is found in the off-diagonal elements of the PICM. Two distinct patterns appear in the matrix depending on the relative position of the source with respect to the SUs. First, when $\Delta d_{ij} = 0$, i.e., the source is equidistant to a pair of SUs, the signals received by the i-th and j-th SU yield maximum correlation. Moreover, assuming an idealized noiseless propagation condition with perfect omnidirectional antennas, $[\mathbf{Q}]_{ii} = [\mathbf{Q}]_{jj} = [\mathbf{Q}]_{ij}$. Second, the received signals at the i-th and j-th SU yield minimum correlation when $\Delta d_{ij} = mR$, i.e., $[\mathbf{Q}]_{ij} \approx 0$, where $m \in \mathbb{Z}^*$ is a nonzero integer, but equality holds if the transmit signal has an Kronecker delta function as its discrete-time periodic autocorrelation function. These two cases are illustrated by Fig. 2, which shows the map of a WSN with a single active source in Fig. 2a, and the corresponding absolute value of the correlation matrix with diagonal entries normalized to the unity in Fig. 2b.

As it is readily apparent, the performance of a positioning algorithm using the PICM as its input will be directly related to its information level, which in turn depends on the system bandwidth, spatial arrangement of the SUs, and the transmit signal correlation characteristics. The highest information level stemming from the off-diagonal elements of PICM arises when the source is located at points where $0 \leq \Delta d_{ij} \leq R$ from the perspective of most SUs. Thus, assuming fixed SU placement, there is an average differential source-SU distance denoted by $\overline{\Delta d_{ij}} = \mathrm{E}\left[|d_i - d_j|\right]$, which can be obtained for each environment, and it depends on the location of the SUs and possible locations where the source may be. The average differential source-SU distance can be used for calculating the system bandwidth that maximizes the positioning information of the correlation matrix as

$$B_{\mathrm{pos}} = \frac{c}{\overline{\Delta d_{ij}}}, \tag{12}$$

which ensures that on average the PICM values are within the first lobe of Fig. 1.

C. Neural Network Architecture

Given the two dimensional image-like structure of the PICM, a convolutional neural network (CNN) architecture is employed for estimating the source location. The CNN takes as input the absolute value of the correlation matrix in logarithm scale, which is here defined as the PICM. The complete list of the architecture hyperparameters employed are presented in Table I, and the network architecture is illustrated in Fig. 3b.

Figure 3a shows the training history, where 3200 training examples are employed for training. Detailed description of the training data is given in section IV-B. It can be observed that a well fitting model is obtained with approximately 300 epochs.

IV. Performance Evaluation

A. RSS- and TDoA-based Positioning Algorithms

1) DNN-RSS: This approach has been proposed in our previous work [9], and further investigated with measurement

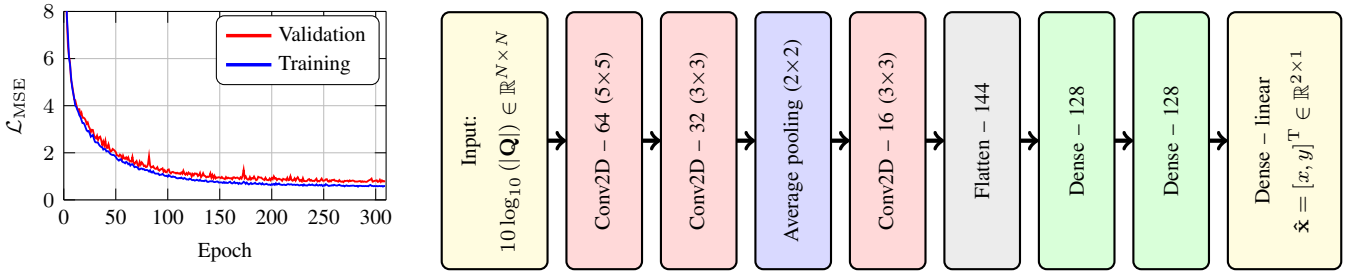

(a) Training history.

(b) Architecture.

Fig. 3: Proposed CNN architecture and mean squared error (MSE) loss as a function of training epochs for training and validation data sets.

TABLE I: Proposed CNN architecture hyperparameters

Hyperparameter	Value
Architecture	Convolutional and FC
Number of convolutional layers	3
Number of kernels	64, 32 and 16
Kernel sizes	(5, 5), (3, 3) and (3, 3)
Padding	Valid
Pooling	Average (2, 2)
Number FC layers	2
Number units per FC layer	128, 128
Number of trainable parameters	≈ 60,000
Validation split	80% training, 20% validation
Mini batch size	40
Regularization parameter (L2)	0.01
Activation function	ELU
Early stop patience	100
Optimizer	Adaptive moments (Adam)
Learning rate	10^{-3}
Loss function	MSE
Weight initialization	Glorot Normal

TABLE II: Simulation parameters

Parameter	Value
Area size	20×20 m^2
Source height	1.5 m
SU height	3.5 m
Number of SUs (N)	16 (Fig. 2a)
Average differential source-SU distance $\left(\overline{\Delta d_{ij}}\right)$	≈ 6.042 m
Positioning bandwidth (B_{pos})	≈ 49.6059 MHz
Average SNR	20 dB
Transmit signal	Zadoff Chu (Eq. (11))
Transmit signal length	256 samples
Transmit and receive antenna radiation pattern	Omnidirectional
Frequency of operation (f_c)	3.75 GHz
Path loss exponent of each ray	2
Maximum number of ray interactions (reflection & diffraction)	3
Number of propagation paths	20
Training set size	3200 examples
Test set size	3200 examples

data [10]. The neural network architecture employed is a fully connected neural network with three hidden layers that takes as input the RSS measurements from the N SUs.

2) NLS- and LLS-TDoA: TDoA is the difference between time of arrival (ToA) estimates at a pair of SUs, where ToA corresponds to the delay that the signal emitted by a source takes to reach a given SU. In scenarios with non-line-of-sight (NLoS) propagation conditions, the performance of delay estimation algorithms suffers with a positive bias, i.e., the estimated delay is greater than the true delay. In turn, the accuracy of time-based positioning schemes is degraded in comparison to LoS conditions.

The nonlinear least squares (NLS) and linear least squares (LLS) estimators using TDoA ranging as input are described in [11] in the chapters 3.3.1.1.B and 3.3.2.1.B, respectively. In this work, the NLS is implemented via grid search with a resolution of 5 cm.

B. Channel Model & Simulation Parameters

In order to understand how the proposed scheme performs, and how does it compare against pure RSS- and TDoA-based techniques, a simulation environment has been built using the ray tracing tool Altair WinProp™ [12], and the numeric computing software MATLAB™. The ray tracing tool allows the creation of channel impulse responses that are naturally associated with unique source locations. Therefore, positioning parameters, e.g., RSS and TDoA, can be obtained from a signal that has been subjected to the same channel impulse response and SNR.

WinProp outputs the propagation paths between transmitter-receiver pairs with a given maximum number of wave interactions for specific positions within the simulated environment, where the reflectivity coefficients dependent on electric properties of the construction materials are taken into account. The area is modeled with concrete floors, brick walls, metal roof, and its dimension is 20 by 20 meters. The area dimensions

similar to a factory hall, where sixteen SUs are positioned following the illustration on Fig. 2a. The propagation paths are calculated at a finite number of positions across the room with a resolution of 0.25 m between adjacent points, which equates to 6400 distinct positions within the area. At each simulation run, one static signal source is generated with coordinates randomly drawn from the 6400 positions without replacement. For training and testing, the entire data set is split into two independent data sets with 3200 points each. WinProp outputs the propagation paths as vectors, which contain the gains, delays and phases associated with a pair of source and receiver locations. The propagation path vectors are then processed by a MATLAB script that calculates the bandlimited received signal at the j-th SU with (5), where the transmit signal is a Zadoff-Chu sequence with 256 samples, and the bandlimited channel frequency response is obtained via (2). The complete list of simulation parameters is shown in Table II.

Two distinct evaluation scenarios have been devised, namely *static* and *dynamic*. In the static setup, besides AWGN, no other source of signal perturbation or distortion is taken into account. Therefore, the performance of the positioning algorithms is affected chiefly by the multipath propagation effects in high SNR regime. The dynamic setup extends the static scenario by weighting each propagation path with a complex normally distributed gain $\xi \sim \mathcal{CN}(0,1)$ for modeling random signal attenuations that come from occasional path blockage due to moving obstacles within the environment. Hence, each path amplitude becomes Rayleigh distributed and each path phase is randomly rotated following a uniform distribution between 0 and 2π. This setup is inspired by the stochastic models often employed in the investigation of wireless communications systems, where agreement with measurements have long been reported in the literature [13].

The proposed CNN-PICM technique is compared against (*i*) deep neural network (DNN)-RSS [9], [10], (*ii*) LLS-TDoA, and (*iii*) NLS-TDoA [11].

C. Static Environment

Figure 4a presents the positioning performance by showing the root mean squared error (RMSE) of the source coordinates as a function of the bandwidth. In this case, one CNN/DNN model was obtained for each bandwidth point, where Fig. 3a shows the training progress of the CNN-PICM approach for $B = B_{\text{pos}}$. Both NLS- and LLS-TDoA improves with increasing bandwidth, since it directly relies on correlation for TDoA estimation, which is in turn limited by the correlation spatial resolution. However, the superior performance of NLS against LLS comes with the cost of impractical computational complexity for realtime deployment. Similarly, DNN-RSS performance also improves as the system bandwidth increases, since the RSS variation resulting from multipath fading is reduced due to the decreasing correlation among propagation paths. As discussed above, CNN-PICM has an ideal operation bandwidth that maximizes the representation of the source position in the correlation matrix, this value is highlighted in the plot. For values where $B \ll B_{\text{pos}}$, CNN-PICM and DNN-RSS have similar performance, since the signals received at all the SUs are highly correlated, and the PICM does not contain extra information in the off-diagonal elements. For $B \gg B_{\text{pos}}$, CNN-PICM and DNN-RSS also show similar performance, however, in this case the correlation among the received signals decays rapidly due to the large bandwidth, and effectively all received signals are highly uncorrelated, and again the PICM does not contain extra information in its off-diagonal. In both situations CNN-PICM still relies on the location information contained in the main diagonal, which corresponds to the RSS. Hence, the similar performance between CNN-PICM and DNN-RSS.

Figure 4b shows the CDF of the positioning error with operation bandwidth given by (12). Giving yet another perspective, Fig. 4c shows the relation between the SNR and the positioning error, this result indicates that the proposed approach performs well under moderate SNR regime, i.e., greater than 10 dB.

D. Dynamic Environment

Figures 5a and 5b are obtained under the dynamic simulation setup. In this case, the training process is not repeated, so the DNN and CNN models trained with the data set from the static environment are employed. As expect, the performance of all schemes deteriorates due to the assumption of random movement within the area. Comparing the results from the two simulation environments it can be noted that DNN-RSS performance remains unaffected by an increasing system bandwidth, since the power fluctuations are now a combined effect from multipath fading and the additional random signal blockage modeled by ξ. On the other hand, NLS- and LLS-TDoA still shows improving performance as the system bandwidth increases, since it relies on the correlation among signals received at the SUs for TDoA estimation, which in turn is not heavily influenced by power fluctuations, but rather by the signal correlation characteristics and the spatial resolution. Moreover, this result shows that despite the random signal fluctuations, CNN-PICM is able to exploit the correlation patterns when the system bandwidth is properly selected, i.e., following (12). Nevertheless, its performance degrades as the bandwidth increases, since in that operating region the source position information is understood to be the RSS contained in its main diagonal. At $B = B_{\text{pos}}$ CNN-PICM presents performance comparable to LLS-TDoA, however requiring about 20 times less bandwidth.

V. Conclusion

In this paper, the CNN-PICM positioning approach is proposed. The scheme employs a CNN to estimate the source coordinates using as input the position information correlation matrix (PICM) obtained from the received signals at spatially distributed and synchronized SUs. Guidelines on how to maximize the PICM positioning information are presented, which are related to the sampling frequency, i.e., system bandwidth, and the auto correlation function of the positioning pilot signal. The performance of the proposed approach is investigated

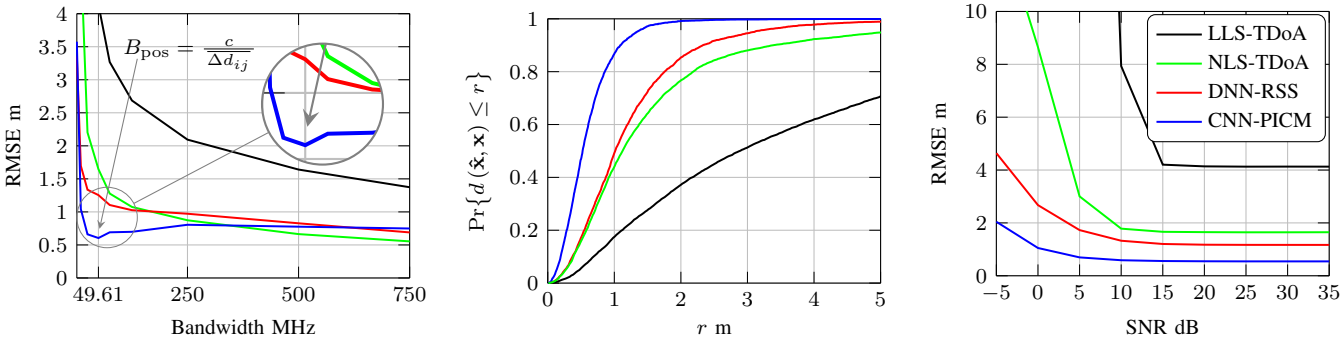

(a) (b) (c)

Fig. 4: Performance under the static simulation scenario. Plot (a) shows the RMSE of the estimated sources coordinates as a function of the bandwidth with SNR = 20 dB. Plot (b) shows cumulative distribution function (CDF) of the positioning error with SNR = 20 dB and $B = B_{\text{pos}} = 49.61$ MHz. Plot (c) shows the RMSE of the estimated sources coordinates as a function of the SNR with $B = B_{\text{pos}} = 49.61$ MHz.

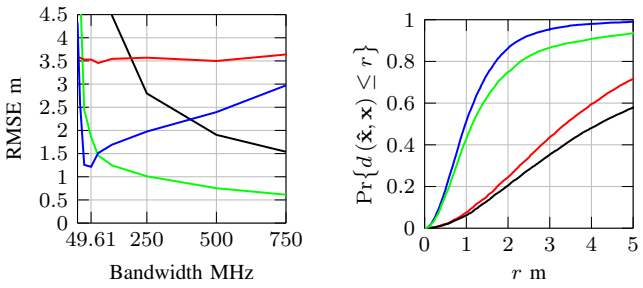

(a) (b)

Fig. 5: Performance under the dynamic simulation scenario. Plot (a) shows the RMSE of the estimated sources coordinates as a function of the bandwidth with SNR = 20 dB; (b) shows CDF of the positioning error with SNR = 20 dB and $B = B_{\text{pos}} = 49.61$ MHz.

using a ray tracing tool. The results give support to the idea of a DL-based technique being able to push the performance of indoor positioning techniques beyond what is currently possible with traditional localization parameters, such as RSS and TDoA, and low complexity estimators, such as the LLS. The proposed approach is able to deliver accurate positioning while being low-complexity and requiring relatively narrow bandwidth. Investigating the proposed approach with real world data is an important next step. Nevertheless, future theoretical studies should also investigate the feasibility of extending the PICM to a three dimensional tensor containing in each page a correlation matrix calculated with different time shifts.

Acknowledgment

This work was supported by the German Federal Ministry of Education and Research (BMBF) under the projects and KOMSENS-6G (16KISK124) and 6G-life (16KISK001K), and by the German Research Foundation (DFG, Deutsche Forschungsgemeinschaft) as part of Germany's Excellence Strategy - EXC 2050/1 - Project ID 390696704 - Cluster of Excellence "Centre for Tactile Internet with Human-in-the-Loop" (CeTI).

References

[1] M. Chafii, L. Bariah, S. Muhaidat, and M. Debbah, "Twelve scientific challenges for 6g: Rethinking the foundations of communications theory," *IEEE Communications Surveys & Tutorials*, vol. 25, no. 2, pp. 868–904, 2023.

[2] A. Behravan, V. Yajnanarayana, M. F. Keskin, H. Chen, D. Shrestha, T. E. Abrudan, T. Svensson, K. Schindhelm, A. Wolfgang, S. Lindberg, and H. Wymeersch, "Positioning and sensing in 6G: Gaps, challenges, and opportunities," *IEEE Vehicular Technology Magazine*, vol. 18, no. 1, pp. 40–48, 2023.

[3] F. Liu, Y. Cui, C. Masouros, J. Xu, T. X. Han, Y. C. Eldar, and S. Buzzi, "Integrated sensing and communications: Toward dual-functional wireless networks for 6g and beyond," *IEEE Journal on Selected Areas in Communications*, vol. 40, no. 6, pp. 1728–1767, 2022.

[4] T. Wild, V. Braun, and H. Viswanathan, "Joint design of communication and sensing for beyond 5G and 6G systems," *IEEE Access*, vol. 9, pp. 30845–30857, 2021.

[5] A. Goldsmith, *Wireless Communications*. Cambridge University Press, 2005.

[6] A. Leon-Garcia, *Probability, Statistics, and Random Processes for Electrical Engineering*. Pearson Education, Inc., 3rd ed. ed.

[7] I. Goodfellow, Y. Bengio, and A. Courville, *Deep Learning*. MIT Press, 2016.

[8] E. García, J. A. Paredes, F. J. Álvarez, M. C. Pérez, and J. J. García, "Spreading sequences in active sensing: A review," *Signal Processing*, vol. 106, pp. 88–105, 2015.

[9] I. B. F. de Almeida, M. Chafii, A. Nimr, and G. Fettweis, "Blind transmitter localization in wireless sensor networks: A deep learning approach," in *2021 IEEE 32nd Annual International Symposium on Personal, Indoor and Mobile Radio Communications (PIMRC)*, pp. 1241–1247, 2021.

[10] I. Bizon, Z. Li, A. Nimr, M. Chafii, and G. P. Fettweis, "Experimental performance of blind position estimation using deep learning," in *GLOBECOM 2022 - 2022 IEEE Global Communications Conference*, pp. 4553–4557, 2022.

[11] H. C. So, *Source Localization: Algorithms and Analysis*, ch. 3, pp. 59–106. 2019.

[12] Altair Engineering, Inc., "Altair WinProp™ - wave propagation and radio network planning," May 2019.

[13] A. Saleh and R. Valenzuela, "A statistical model for indoor multipath propagation," *IEEE Journal on Selected Areas in Communications*, vol. 5, no. 2, pp. 128–137, 1987.